Modeling of Ultrafast Heat- and Field-Assisted Magnetization Dynamics in FePt

P. Nieves and O. Chubykalo-Fesenko

Instituto de Ciencia de Materiales de Madrid, CSIC, Cantoblanco, 28049 Madrid, Spain

(Received 12 August 2015; revised manuscript received 26 October 2015; published 19 January 2016)

The switching of magnetization by ultrafast lasers alone in FePt could open a technological perspective for magnetic recording technology. Recent experimental results [D. Lambert *et al.*, Science 345, 1337 (2014)] indicate a dynamical magnetization response in FePt under circularly polarized laser pulses. Using high-temperature micromagnetic modeling, based on the stochastic Landau-Lifshitz-Bloch equation, we investigate the possibility of magnetization switching in FePt under the action of an ultrafast heat pulse assisted by either a constant or optomagnetic field. We evaluate the necessary magnitude and duration of the inverse Faraday field to produce a reliable switching. Our results also reproduce experimentally observed magnetization patterns originated from the nonhomogeneous temperature distribution.

DOI: 10.1103/PhysRevApplied.5.014006

I. INTRODUCTION

The FePt $L1_0$ alloy represents the most important material for concepts in magnetic recording due to its high magnetic anisotropy, which is responsible for long-time thermal stability of nanometer-sized bits. Thin films of FePt with perpendicular anisotropy and small grain sizes are the most promising candidates for heat-assisted magnetic recording (HAMR), an already-working technology which incorporates laser heating into the recording process [1–3]. HAMR together with patterning of individual bits in high-anisotropy materials such as FePt can, in principle, extend recording densities to 100 Tb/in^2.

On the other hand, the ultimate magnetic recording applications will also require faster bit switching. Recently, it has been shown that proper heat-sink layers optimize the recording-time window down to 0.1–0.2 ns in HAMR of granular FePt media [4]. The challenge of achieving even shorter recording-time windows has led to an intensive investigation of the ultrafast magnetization dynamics. The possibilities are opened by the discovery of all-optical switching (AOS) in magnetic materials such as ferrimagnetic alloys and antiferromagnetically coupled multilayers GdFeCo [5], TbCo [6,7], HoCo [7], or TbFe [8]. Recently, AOS has been observed in ferromagnetic multilayers such as Co/Pt [9].

The main mechanism for the AOS in ferrimagnetic alloys is based on the nonequivalent thermodynamical response of the two sublattices and the angular momentum transfer between them [10,11]. This mechanism cannot occur in single-phase materials such as FePt. Neither can it be envisaged to be produced in ferromagnetically coupled alloys and multilayers.

The possibility of AOS in FePt and CoPt could open extraordinary perspectives for the future of magnetic recording. The AOS potentially can not only extend the magnetization switching to ultrafast time scales and remove the recording head requirement, but also present advantages from the point of view of energy saving [12], especially compared to HAMR. The first experimental measurements of the laser-induced magnetization dynamics in FePt [13] show that this material does not switch even under very intense laser pulses; instead, it shows a slow magnetization recovery owed to the role of critical fluctuations. In 2012, Mendil [14,15] presented systematic experimental measurements of the ultrafast magnetization dynamics in FePt $L1_0$ thin films showing the transition from type-I behavior (fast magnetization recovery) to type-II (slow magnetization recovery) at high fluencies using ultrashort linearly polarized laser pulses. This fact clearly shows that a pure heat-assisted magnetization reversal does not occur in FePt. This also could establish a speed limit of the magnetic recording in FePt media [15].

However, in 2014, Lambert *et al.* [9] showed that ultrashort circularly polarized laser pulses can induce a small helicity-dependent magnetization in demagnetized samples of FePtAgC granular film. This result has posed a question about the possibility of AOS magnetic recording in FePt media where the use of an external magnetic field may not be necessary during the writing process. The debate on the origin of this phenomena is still going on, and more experiments are clearly necessary in order to clarify if FePt could be switched on the ultrafast time scale without the need of any applied field or with the help of a small one. The only mechanism which has been discussed to be possibly responsible for such switching is the field coming from the inverse Faraday effect [5], previously also discussed in ferrimagnetic alloys where the helicity-dependent switching is also widely observed [6–9].

In the present article, we investigate theoretically the requirements to switch FePt in the presence of the heat pulse produced by the laser and assisted by either a constant or ultrafast optomagnetic field. The latter is assumed to be

originated by the inverse Faraday effect, as in previous work [12,16–18].

In order to describe the ultrafast magnetization dynamics of a FePt thin film at a large spatial scale, we consider a high-temperature micromagnetic model based on the stochastic quantum Landau-Lifshitz-Bloch (LLB) equation [19,20] coupled to the two-temperature model (2TM) [21]. For the 2TM, we use parameter set I given in Ref. [15], which gives a good agreement with previous experimental results in this material. Particularly, this parameter set shows that the electron-specific heat in FePt is influenced by the noble character of Pt and is around 10 times smaller than in transition metals. As a consequence, the electronic temperature peak is of the order of 1500 K for the highest pulse fluencies, and the temperatures are close to the Curie temperature of FePt when electron and phonon temperatures are equilibrated. Such high temperatures should influence the ultrafast magnetization dynamics and facilitate magnetization switching in comparison to, for example, Ni. One of the goals of the present article is to investigate the consequence of such a high temperature.

In Sec. II of the present article, we present the results of the modeling of magnetization dynamics under an ultrafast laser pulse and a constant magnetic field. In Sec. III, the constant magnetic field is substituted by the ultrafast optomagnetic field with different magnitude and duration. The modeling is done on continuous and granular thin film also considering spatially nonhomogeneous laser heating, which reproduce experimentally observed spatially nonhomogeneous switching patterns. Section IV concludes the article.

II. ULTRAFAST MAGNETIZATION DYNAMICS IN CONSTANT EXTERNAL MAGNETIC FIELDS

The ultrafast laser-induced magnetization dynamics in FePt under constant and moderate external magnetic fields is very relevant to the heat-assisted magnetic recording. We consider first the case of a continuous FePt magnetic film. The details of the LLB-based micromagnetic model and the system parameters that we use in our simulations are given in Refs. [15,22]. Namely, we assume the temperature-dependent saturation magnetization, anisotropy, and exchange parameters, scaled with magnetization which followed from the multiscale description of the magnetization dynamics in FePt [23,24]. The micromagnetic model dynamics is governed by the LLB equation with spin $S = 3/2$ and thermal fluctuations coming from the electron temperature of the 2TM. Periodic boundary conditions in the x and y axes are considered.

We consider that the initial magnetization is saturated in the up direction (perpendicular to the thin film which is in the xy plane). First, we saturate the magnetization in the up direction (perpendicular to the thin film) and equilibrate the magnetization during 500 ps without an applied field at $T = 300$ K, then the magnetization is equilibrated with an applied field in the opposite direction during 100 ps, and finally the pulse is applied, keeping the external field on. To investigate the limiting reversal conditions and the influence of the high electronic temperatures in FePt, we use the highest pump fluencies up to $F = 50$ mJ/cm^2 available in the experiment [15]. Note that the actual fluence value may change in different experimental conditions, scaled by the amount of the absorbed energy. In Fig. 1, we present the magnetization dynamics in the continuous film under the laser-pulse excitation with $F = 40$ mJ/cm^2 for different field values. We see that the switching of the magnetization takes place for the applied fields $\mu_0 H_z = -3$ and -5 T with the limiting switching field slightly below $\mu_0 H_z = -1$ T, where μ_0 is the permeability of free space. For comparison, the anisotropy field is 4.4 T at room temperature; i.e., the fields of the magnitude smaller than that do not reverse the magnetization without the laser (ultrafast heat) pulse at stationary conditions. Note also that

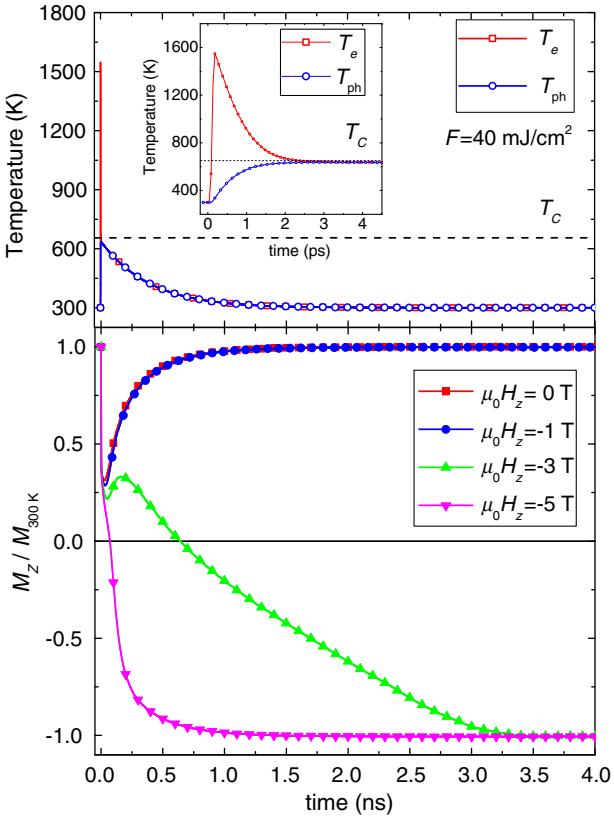

FIG. 1. (Top) Electron- and phonon-temperature dynamics with a laser-pulse fluence $F = 40$ mJ/cm^3. The inset shows electron- and phonon-temperature dynamics during the first picoseconds. (Bottom) Normalized average z component of the magnetization (m_z) versus time in the continuous FePt film model for different applied fields along the z axis: $\mu_0 H_z = 0$, -1, -3, and -5 T. Before the laser pulse, the system is first equilibrated at $T = 300$ K without an external field during 500 ps and then equilibrated with an applied field during 100 ps.

the typical heat-pulse duration of HAMR is longer than that of the ultrafast laser (of the order of 1 ps).

As expected, we observe that the reversal time t_{rev} (defined as the time elapsed between the initial state and the instant of time at which the z component of the mean magnetization begins to reverse its direction, i.e., crosses the $m_z = 0$ point) for each case is very different, ranging from 20 to 200 ps. The dependence of the switching times on the laser-pulse fluency is presented in Fig. 2 for several values of the applied field.

In the magnetization dynamics of the continuous film, we should distinguish two different situations. In the first case, corresponding to the switching time above 100 ps, the dynamics has characteristics of the nonhomogeneous precessional switching, since there is a small average perpendicular magnetization component. The typical magnetization configurations (in this case, under the field $\mu_0 H_z = -3$ T and the laser fluency $F = 40$ mJ/cm^2) presented in Figs. 3(a) and 3(b) show the creation of perpendicular domains. While the temperature is cooled down, these domains grow in size and shrink, leading finally to a bubblelike structure [see Figs. 3(c) and 3(d)] which is stable during a long time period until it disappears completely at $t \simeq 4$ ns. We evaluate the propagation velocity of the bubble of the order of $v \simeq 250$ m/s.

On the other hand, at high fluencies or a strong external applied field of $\mu_0 H_z = -5$ T, the reversal time is below 100 ps. Here the large magnetization domains are not formed (see Fig. 4). Instead, the initial part of the reversal is almost linear on both each macrospin (decrease of the local magnetization magnitude) and average magnetization (no average perpendicular component) level. Many small bubblelike structures randomly nucleate, coalesce, and disappear.

Thus, we estimate that the magnetization in continuous FePt thin films could be reversed by using a powerful ultrashort linearly polarized pulse and a static applied field larger than 1 T. However, this reversal is ultrafast only for fields close to 5 T or large temperatures.

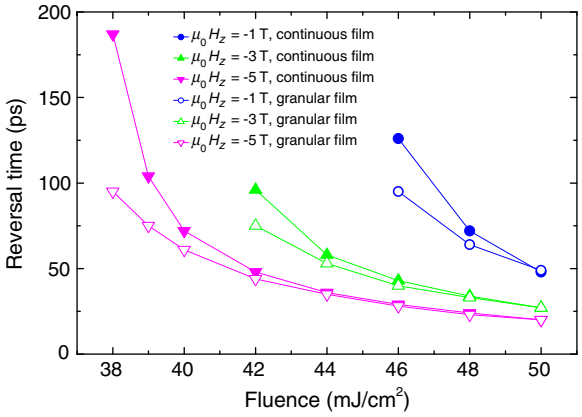

FIG. 2. Typical values of the reversal time as a function of the laser pump fluency for several values of the applied field. The solid symbols correspond to the continuous field simulations while the open ones to the granular film.

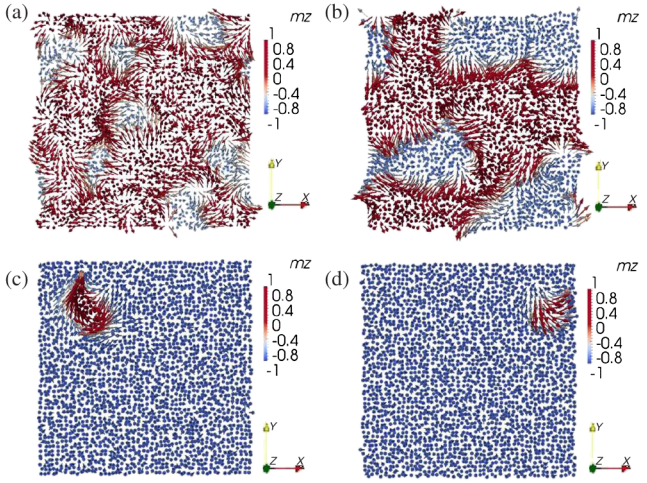

FIG. 3. Snapshots of the system magnetization state in the continuous film with $F = 40$ mJ/cm^3 and $\mu_0 H_z = -3$ T at time moments (a) $t = 0.25$ ns, (b) $t = 0.5$ ns, (c) $t = 3.2$ ns, and (d) $t = 3.6$ ns. The figures show an area of 150×150 nm.

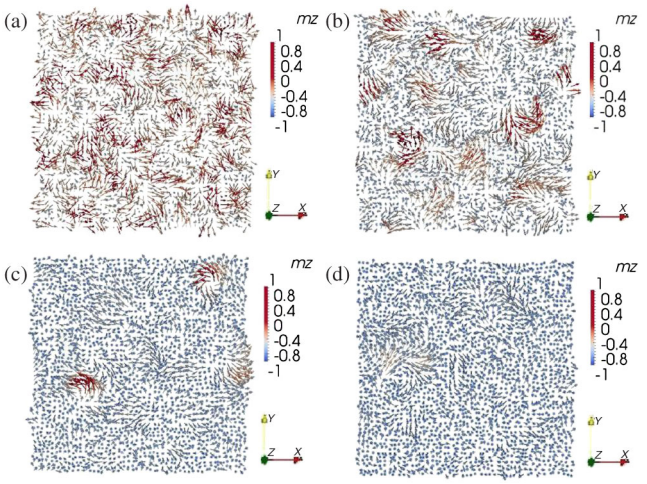

FIG. 4. Snapshots of the system magnetization state in the continuous film with $F = 40$ mJ/cm^3 and $\mu_0 H_z = -5$ T at time moments (a) $t = 0.11$ ns, (b) $t = 0.15$ ns, (c) $t = 0.21$ ns, and (d) $t = 0.24$ ns. The figures show an area of 150×150 nm.

In order to simulate the magnetization dynamics of a FePt granular thin film, we consider a simplified model with a collection of grains interacting with a low exchange value $A_i(0) = 2.2 \times 10^{-8}$ erg/cm, that is, 100 times smaller than in the continuum film model. The temperature dependence of the parameters is considered the same as in the continuous case. As is expected, the dynamics of this model is very different, since low exchange interaction forbids the formation of the collective magnetization structures such as domain walls or bubbles.

Consequently, the grains switch almost independently. The typical switching time of an individual grain is larger than that of the continuous films, since magnetization nucleation and propagation are not allowed. At the same time, the reversal times of a collection of grains is slightly smaller than in the continuous media; see Fig. 2. This happens because in the granular media to achieve the magnetization $m_z = 0$ the switching of all grains is not necessary. At high fluencies, however, i.e., high temperatures, when the magnetization dynamics is practically linear, the reversal time of a continuous and a granular film are almost the same, since at high temperatures the macrospins are decoupled in both cases.

In conclusion, the intergranular exchange interactions play a role at the time scale of 100 ps, making the response of continuous and granular media different. At a high pump fluency, however, their role is negligible. The magnetostatic interactions do not play any significant role in the magnetization dynamics in this time scale.

III. ALL-OPTICAL CONTROL OF THE MAGNETIZATION USING CIRCULARLY POLARIZED LASER PULSES

Recently, an all-optical control of the magnetization using circularly polarized laser pulses in FePt thin films has been observed [9]. Unfortunately, in this experimental work no magnetization as a function of time is measured, and only the final magnetization state is presented. Therefore, it is not completely clear whether the results presented can be attributed to the ultrafast magnetization dynamics produced by the laser pulse or to the influence of the superparamagnetic behavior occurring on a larger time scale. In this section, we investigate the effect of ultrashort circularly polarized laser pulses on continuous and granular FePt thin films.

A. Modeling magnetization dynamics under the inverse Faraday effect

Motivated by the results of Ref. [9], we investigate the conditions where circularly polarized laser pulses can produce a magnetization reversal in continuous and granular FePt thin films. Similar to Ref. [18], we include the effect of the circularly polarized laser pulse (inverse Faraday effect) as a light-induced effective magnetic field of the form

$$\mathbf{H}_{\mathrm{OM}}(t) = \sigma H_{\mathrm{OM}}^{\max} f(t)\mathbf{n}, \tag{1}$$

where $\mathbf{n}$ is the unit vector in the direction of the wave vector light and σ gives the sense of circular polarization and is equal to ± 1 and 0 for right- (σ^+) or left-handed (σ^-) circularly polarized and linearly polarized light, respectively. $H_{\mathrm{OM}}^{\max}$ is the maximum value that the light-induced effective field can achieve, and we use it as a parameter in our simulations. The function $f(t)$ is given by [18]

$$f(t) = \begin{cases} e^{-(t/\tau)^2}, & t < 0, \\ e^{-[t/(\tau+2\tau_{\mathrm{decay}})^2]}, & t > 0, \end{cases} \tag{2}$$

where τ is the pulse duration with a value of $\tau = 40$ fs and τ_{decay} is a parameter, defining the decay time of the inverse Faraday effect (IFE). In the stationary situation, the electromagnetic field coming from the laser is proportional to the laser intensity [16,25]. Here we assume that the inverse Faraday field comes from the nonequilibrium electronic excitation, and, thus, similar to Ref. [18], we assume that it lasts somewhat longer than the laser pulse. In order not to mix the effect of increasing temperature and IFE field, we assume the fluency and the maximum IFE field as independent parameters. If the IFE field is proportional to the fluency, then fluency values assumed here should be renormalized by the corresponding factor. Notice that, since the laser pulse is applied perpendicular to the film plane (xy), we have $\mathbf{n} = -\mathbf{e}_z$. Therefore, right-handed ($\sigma^+ = \sigma = +1$) circularly polarized light induces an optomagnetic field where its z component $H_{\mathrm{OM},z}$ is negative, while left-handed ($\sigma^- = \sigma = -1$) polarization leads to an optomagnetic field where $H_{\mathrm{OM},z}$ is positive.

B. Continuous film

First, we simulate the magnetization dynamics of a continuous FePt thin film using the same micromagnetic model, where we substitute the constant magnetic field by the optomagnetic field given by Eq. (1) with variable duration. We use a right-handed circularly polarized laser pulse ($\sigma = +1$) where the direction of the wave vector is perpendicular to the thin film ($\mathbf{n} = -\mathbf{e}_z$). Therefore, the optomagnetic field points in the opposite direction to the initial magnetization.

In Fig. 5(a), we show the dynamics of the magnitude of the optical-magnetic field $|\mathbf{H}_{\mathrm{OM}}|$ induced by a right-handed circularly polarized laser pulse with $\mu_0 H_{\mathrm{OM}}^{\max} = 23$ T and different values of the parameter τ_{decay} (upper panel), the dynamics of the electron and phonon temperatures (middle panel), and the corresponding magnetization dynamics (lower panel) for FePt (parameter set I given in Ref. [15], low electron-heat-capacity case) and a fluence of $F = 40$ mJ/cm^2. Here a magnetization reversal is observed for the cases $\tau_{\mathrm{decay}} = 10$–$50$ ps. In Fig. 5(b), we present the same simulations as in Fig. 5(a) but assuming a higher electron-heat capacity ($C_e = \gamma_e T_e$); namely, we set $\gamma_e = 1100$ J/m^3 K^2. As a consequence, the electronic temperature is lower than in the previous case, and the same optomagnetic field cannot reverse the magnetization. These electronic temperatures are more proper for transition metals, such as for Ni. Therefore, we conclude that high electronic temperatures in FePt may help the switching of the magnetization using circularly polarized laser pulses.

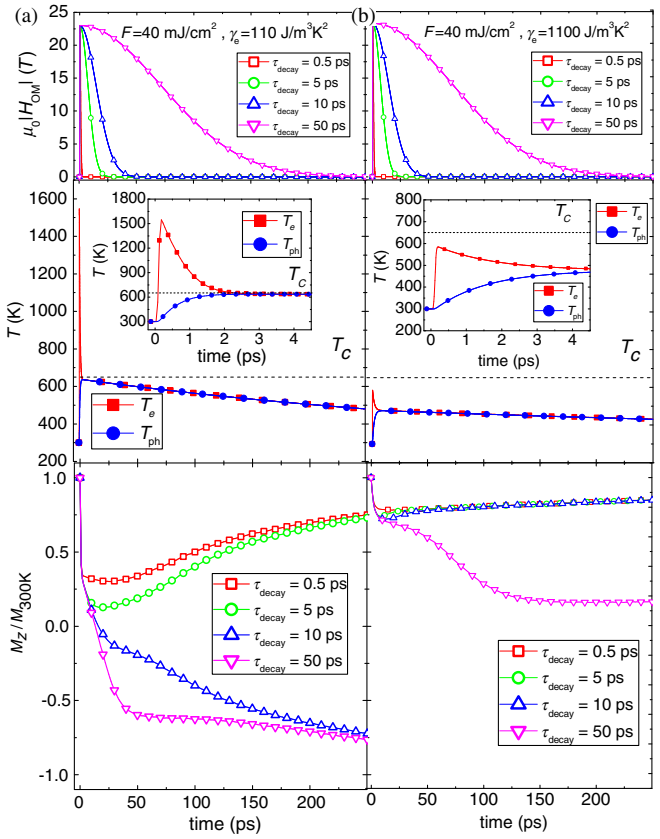

FIG. 5. The dynamics of the magnitude of the optical-magnetic field $|\mu_0 \mathbf{H}_{\mathrm{OM}}|$ ($\mu_0 H_{\mathrm{OM}}^{\max} = 23$ T) induced by a right-handed circularly polarized laser pulse (upper panel), the corresponding dynamics of the electron and phonon temperature (middle panel), and the magnetization dynamics in the continuous film (lower panel) under the laser pulse with the fluence $F = 40$ mJ/cm^2 (a) using the parameters for the 2TM with electronic-specific heat coefficient $\gamma_e = 110$ J/m^3 K^2 corresponding to FePt of the present article (the parameter of set I given in Ref. [15]) and (b) using the parameters for the 2TM proper for transition metals with electronic-specific heat coefficient $\gamma_e = 1100$ J/m^3 K^2. The insets show the electron- and phonon-temperature dynamics during the first picoseconds.

Next, we evaluate the region of the parameters (amplitude and decay time of the optomagnetic field) where the magnetization reversal takes place; see Fig. 6. For this task, we perform similar simulations as in Fig. 5 for different values of the optical-magneto parameters $H_{\mathrm{OM}}^{\max}$ and τ_{decay} using the highest available fluence equal to $F = 50$ mJ/cm^2. It may be seen that the reversal occurs for either field amplitudes larger than 10 T or the inverse Faraday duration of the order of 10 ps. If the decay time of the inverse Faraday effect is of the order of 0.5 ps, its necessary magnitude is of the order of 40 T. The magnitude and duration of the optomagnetic field needed to reverse the magnetization may be too large, and perhaps they may not be achieved through the inverse Faraday effect. However, very recent *ab initio* estimations of the inverse Faraday field

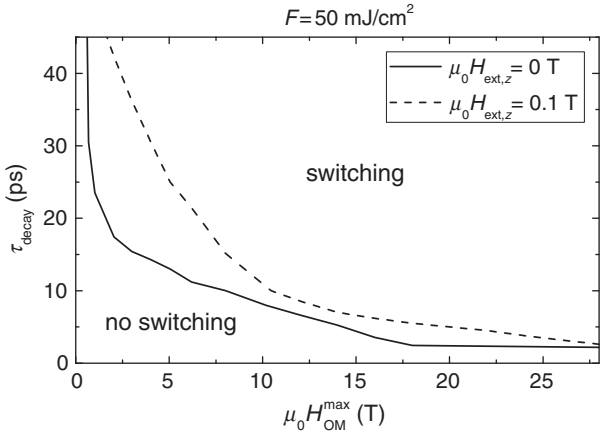

FIG. 6. Phase diagram showing for which optical-magnetic parameters ($H_{\mathrm{OM}}^{\max}$ and τ_{decay}) the magnetization switching is achieved in the continuous film. A solid line separates switching and no-switching regions for the case of zero external magnetic field, and the dashed line for the case with an external magnetic field $\mu_0 H_z = 0.1$ T in the same direction of the initial magnetization and opposite to the optomagnetic field $\mathbf{H}_{\mathrm{OM}}$ induced by a right-handed (σ^+) circularly polarized laser pulse.

suggest that this optomagnetic field may be indeed very strong [26].

Now, we would like to investigate if a small but constant external magnetic field of the order of 0.1 T can prevent the magnetization switching when a circularly polarized laser pulse is applied to a continuous FePt thin film, as it is observed experimentally in granular samples [9]. For this task, we perform similar simulations with a constant external magnetic field equal to $\mu_0 H_z = 0.1$ T pointing in the same direction as the initial magnetization, that is, opposite to the optomagnetic field $\mathbf{H}_{\mathrm{OM}}$ induced by a right-handed (σ^+) circularly polarized laser pulse. The results are presented in Fig. 6, where switching and no-switching regions are separated by a solid line in the case of no constant external magnetic field and by a dashed line in the case with a constant external magnetic field equal to $\mu_0 H_z = 0.1$ T. We observe that indeed there is a region of parameters where the constant external magnetic field can prevent the magnetization switching under a much stronger but very fast inverse Faraday effect field.

C. Granular film

The experiments in Ref. [9] are made on granular magnetic film. This fact may be important for understanding the optomagnetic switching, since statistically only part of the grains are observed to switch their magnetization. Similar to the experiments described in Ref. [9], we consider an initially demagnetized system; that is, first we randomly assign the grains the directions with up or down magnetization, and then the system is thermalized at room temperature ($T = 300$ K). Note that, strictly speaking, to start with the demagnetized film and to

remagnetize may be somewhat different than to switch it starting from the saturation. It is true that in the case of noninteracting grains both situations involve switching of individual grains. However, due to different interactions, the effects of a temperature decrease or increase could be different for the two cases, especially close to T_c.

We investigate the influence of the electronic temperature dynamics on the magnetization dynamics for a given optomagnetic field. For this task, we simulate three cases with fluencies of $F = 30$, 40, and 50 mJ/cm^2, and in each case we use the same optomagnetic field with $\mu_0 H_{\rm OM}^{\rm max} = 40$ T and $\tau_{\rm decay} = 1$ ps [see Fig. 7(a)]. In Fig. 7(b), we show the time evolution of the spatially averaged value of the z-component magnetization $\langle m_z \rangle$ for each fluency case. The initial increase and subsequent decrease of $\langle m_z \rangle$ observed in all fluency cases are mainly due to the different in-field longitudinal relaxations between the magnetization grains which point to the optomagnetic field and opposite to it; that is, the magnitude of macrospins pointing to the optomagnetic field is larger than the ones pointing opposite to it. In the case $F = 30$ mJ/cm^2 very few grains reverse their magnetization during the dynamics, while for $F = 40$ mJ/cm^2 more grains than in the previous case reverse their magnetization; this process takes place at an approximately constant rate during the time interval 10–60 ps. In the case $F = 50$ mJ/cm^2 the magnetization of some grains initially switches but then slowly reverses again, so that at $t \simeq 60$ ps there are almost the same number of grains where their magnetization point to the down direction as in the initial demagnetized state. As a result, we see that for the same optomagnetic field magnitude there is an optimum electronic temperature dynamics ($F = 40$ mJ/cm^2) where a higher magnetization is achieved at a long time scale.

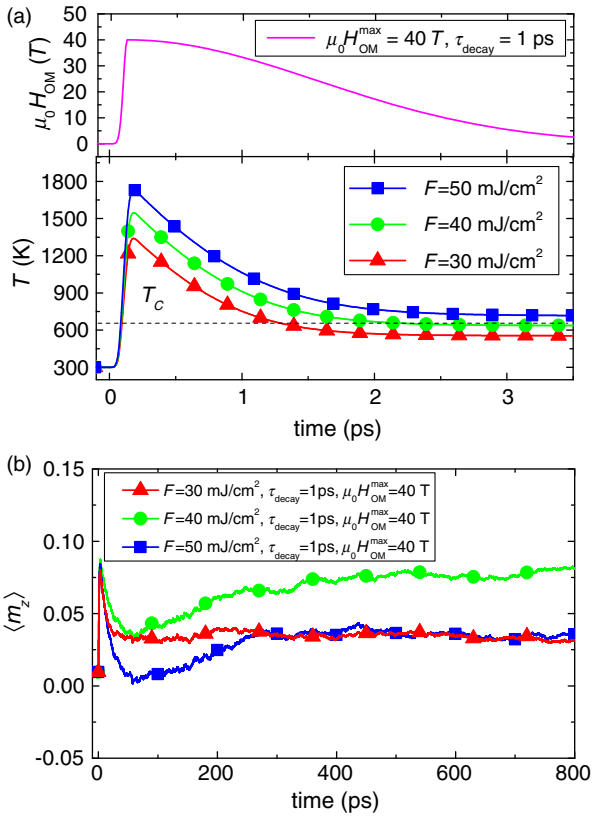

FIG. 7. (a) (top) Optomagnetic field time evolution for $\mu_0 H_{\rm OM}^{\rm max} = 40$ T and $\tau_{\rm decay} = 1$ ps and (bottom) electronic temperature for fluencies of $F = 30$ (red line), 40 (green line), and 50 mJ/cm^2 (blue line). (b) Magnetization dynamics in the granular film corresponding to fluencies of $F = 30$ (red line), 40 (green line), and 50 (blue line) with an optomagnetic field with parameters $\mu_0 H_{\rm OM}^{\rm max} = 40$ T and $\tau_{\rm decay} = 1$ ps.

As was previously discussed [11] for ultrafast demagnetization-remagnetization-switching, a certain amount of energy is necessary. However, too much energy brings the system close to and above the Curie point on a large time scale. In this situation, the dynamics is slow due to the critical fluctuations, and the zero magnetization does not couple well to the external field. In particular, as shown in Fig. 3 of Ref. [27], the dependence of the longitudinal relaxation time $\tau_\parallel$ on the external field (in this case, optomagnetic field) is sharply localized at $T = T_c$, where $\tau_\parallel (T = T_c) \propto 1/H^{2/3}$; that is, the larger the external field is, the lower $\tau_\parallel$ is (slower longitudinal relaxation). Notice that in the case $F = 30$ mJ/cm^2 the electronic temperature crosses T_c very rapidly [see Fig. 7(a)], while in the case $F = 50$ mJ/cm^2 the electronic temperature crosses T_c slowly but at time scales larger than 6 ps where the optomagnetic field is very small. On the other hand, in the case of $F = 40$ mJ/cm^2 the electronic temperature crosses T_c slowly ($t \simeq 1.5 - 6$ ps) when the optomagnetic field is still large. Therefore, in the case $F = 40$ mJ/cm^2 the in-field longitudinal relaxation is longer than in the other fluency cases; this fact could increase the probability of the magnetization reversal. Thus, in terms of the laser fluency, there is a window for the optimum value where the maximum remagnetization occurs.

So far, we have considered a spatially homogeneous electronic temperature and optomagnetic field distributions in our simulations. Now, we repeat the same simulations as in Fig. 7 but with an electronic temperature following spatially a Gaussian distribution $\exp\{-[(\mathbf{r} - \mathbf{r}_0)^2]/a^2\}$, where $\mathbf{r}_0$ is the position of the central point in the laser spot, $\mathbf{r}$ is the position on the film, and $a = 1.2$ μm. Note that the spot size is much smaller than in the experiment but allows one to investigate the effect of the temperature profile. In Figs. 8(a), 8(c), and 8(e), we show snapshots of the electronic temperature distribution at the instant when the electronic temperature reaches its maximum value ($t \simeq 0.2$ ps) for fluencies of $F = 30$, 40, and 50 mJ/cm^2, respectively.

As a consequence of the spatially inhomogeneous electronic temperature, the averaged magnetization $\langle m_z \rangle$ exhibits also a spatially inhomogeneous distribution. This

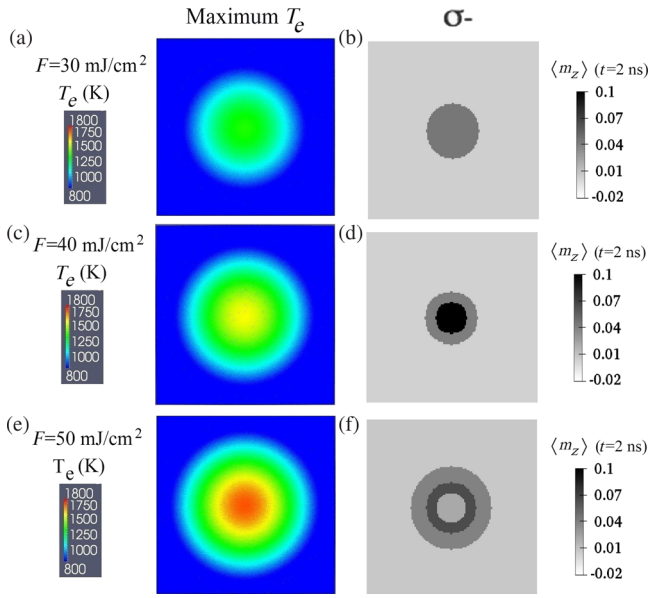

FIG. 8. Snapshots of the electronic temperature assuming a spatially Gaussian distribution for fluencies (a) 30, (c) 40, and (e) 50 mJ/cm^2 at the instant where the electronic temperature reaches its maximum value ($t \simeq 0.2$ ps). The spatial mean value of the z component of the magnetization in the granular film at instant $t = 2$ ns for fluencies (b) 30, (d) 40, and (f) 50 mJ/cm^2. These numerical result figures show an area of 360 × 360 nm.

is shown in Figs. 8(b), 8(d), and 8(f) at instant $t = 2$ ns for fluencies of $F = 30$, 40, and 50 mJ/cm^2, respectively. We see that the smallest fluence ($F = 30$ mJ/cm^2) leads to a small magnetized spot in the center where $\langle m_z \rangle \simeq 0.06$ [see Fig. 8(b)]. The intermediate fluence ($F = 40$ mJ/cm^2) leads to a higher magnetized spot in the center where $\langle m_z \rangle \simeq 0.1$ [see Fig. 8(d)]. The highest fluence ($F = 50$ mJ/cm^2) leads to a magnetized ring where $\langle m_z \rangle \simeq 0.08$ [see Fig. 8(f)]. We see that the grain magnetization can be reversed more efficiently by the optomagnetic field in the regions where the maximum electronic temperature is close to 1500 K. According to Ref. [14], a laser-pulse fluence of $F = 30$ mJ/cm^2 in our simulations corresponds to an experimental measured average power per pulse of $P_{\text{pulse}} = 1.34$ μW, $F = 40$ mJ/cm^2 is equivalent to $P_{\text{pulse}} = 1.79$ μW, and $F = 50$ mJ/cm^2 corresponds to $P_{\text{pulse}} = 2.24$ μW, which are of the same order of magnitude as the P_{pulse} used in Ref. [9]. These results are also in qualitatively good agreement with the experiments presented in Ref. [9]. However, for a more precise comparison, it is necessary to perform a careful analysis of the experiments in Refs. [9,14].

IV. CONCLUSIONS

In summary, we model laser (heat)-induced magnetization dynamics in FePt assisted by either a constant or ultrafast optomagnetic field, produced by the inverse Faraday effect. Our numerical results show that a small electron's specific heat may be an important requirement in order to observe magnetization switching using circularly polarized laser pulses. Therefore, we think that the low electron's specific heat of the FePt favors its all-optical control. We estimate that the optomagnetic inverse Faraday field required to reverse the magnetization in continuous FePt thin films should have a magnitude between 10 (10-ps decay time) and 40 T (0.5-ps decay time). At the same time, only a 0.1-T constant external field could prevent the magnetization reversal induced by the fast and much stronger optomagnetic inverse Faraday field.

In the case of a granular FePt thin film, we find that for a given optomagnetic pulse there is an optimum electronic temperature dynamics, where a maximum number of magnetic grains are reversed. As a consequence, a spatially Gaussian distribution of the electronic temperature favors the formation of a magnetized spot at a low fluence and a magnetized ring at a high fluence, as is observed in the experiments [9].

We would like to point out that the question whether the magnetization dynamics in FePt could be controlled on the ultrafast time scale is still open. The magnitudes of the optomagnetic field which we find in our modeling may be too large for real situations, although we stress again that preliminary *ab initio* calculations show that this might be the case. More experiments in the future should clarify the situation.

Finally, we mention that our model is oversimplified in many senses. Besides the magnitude of the inverse Faraday field, the occurrence of many effects is either unknown or not taken into account properly. This includes the possible heat and electron transport, as well as the proper media characteristics such as the realistic grain size and magnetic parameter distributions. The influence of these effects will be taken into account in subsequent publications.

ACKNOWLEDGMENTS

This work is supported by the Ministerio de Economía y Competitividad (Spain) under Grant No. MAT2013-47078-C2-2-P and by the European Community's Seventh Framework Program (FP7/2007-2013) under Grant Agreement No. 281043, FEMTOSPIN.

[1] M. H. Kryder, E. C. Gage, T. W. McDaniel, W. A. Challener, R. E. Rottmayer, G. Ju, Y.-T. Hsia, and M. F. Erden, Heat assisted magnetic recording, Proc. IEEE **96**, 1810 (2008).

[2] X.Wang, K.Gao, H. Zhou, A. Itagi, N. Seigler, and E. Cage, HAMR recording limitations and extendibility, IEEE Trans. Magn. **49**, 686 (2013).

[3] W. A. Challener, Chubing Peng, A. V. Itagi, D. Karns, Wei Peng, Yingguo Peng, XiaoMin Yang, Xiaobin Zhu, N. J. Gokemeijer, Y.-T. Hsia, G. Ju, Robert E. Rottmayer,

Michael A. Seigler, and E. C. Gage, Heat-assisted magnetic recording by a near-field transducer with efficient optical energy transfer, Nat. Photonics **3**, 220 (2009).

[4] D. Weller *et al.*, in *Sub-nanosecond Heat Assisted Magnetic Recording of FePt Media*, Ultrafast Magnetism I (Springer, New York, 2015).

[5] C. D. Stanciu, F. Hansteen, A. V. Kimel, A. Kirilyuk, A. Tsukamoto, A. Itoh, and Th. Rasing, All-Optical Magnetic Recording with Circularly Polarized Light, Phys. Rev. Lett. **99**, 047601 (2007).

[6] S. Alebrand, U. Bierbrauer, M. Hehn, M. Gottwald, O. Schmitt, D. Steil, E. E. Fullerton, S. Mangin, M. Cinchetti, and M. Aeschlimann, Subpicosecond magnetization dynamics in TbCo alloys, Phys. Rev. B **89**, 144404 (2014).

[7] S. Mangin, M. Gottwald, C-H. Lambert, D. Steil, V. Uhlir, L. Pang, M. Hehn, S. Alebrand, M. Cinchetti, G. Malinowski, Y. Fainman, M. Aeschlimann, and E. E. Fullerton, Engineered materials for all-optical helicity-dependent magnetic switching, Nat. Mater. **13**, 286 (2014).

[8] A. Hassdenteufel, B. Hebler, C. Schubert, A. Liebig, M. Teich, M. Aeschlimann, M. Helm, M. Albrecht, and Rudolf Bratschitsch, Thermally assisted all-optical helicity dependent magnetic switching in amorphous $Fe_{100-x}Tb_x$ alloy films, Adv. Mater. **25**, 3122 (2013).

[9] C.-H. Lambert, S. Mangin, B. S. D. Ch. S. Varaprasad, Y. K. Takahashi, M. Hehn, M. Cinchetti, G. Malinowski, K. Hono, Y. Fainman, M. Aeschlimann, and E. E. Fullerton, All-optical control of ferromagnetic thin films and nanostructures, Science **345**, 1337 (2014).

[10] T. A. Ostler, J. Barker, R. F. L. Evans, R. W. Chantrell, U. Atxitia, O. Chubykalo-Fesenko, S. El Moussaoui, L. Le Guyader, E. Mengotti, L. J. Heyderman, F. Nolting, A. Tsukamoto, A. Itoh, D. Afanasiev, B. A. Ivanov, A. M. Kalashnikova, K. Vahaplar, J. Mentink, A. Kirilyuk, Th. Rasing, and A. V. Kimel, Ultrafast heating as a sufficient stimulus for magnetization reversal in a ferrimagnet, Nat. Commun. **3**, 666 (2012).

[11] J. Barker, U. Atxitia, T. A. Ostler, O. Hovorka, O. Chubykalo- Fesenko, and R. W. Chantrell, Two-magnon bound state causes ultrafast thermally induced magnetisation switching, Sci. Rep. **3**, 3262 (2013).

[12] A. Kirilyuk, A. V. Kimel, and Th. Rasing, Laser-induced magnetization dynamics and reversal in ferrimagnetic alloys, Rep. Prog. Phys. **76**, 026501 (2013).

[13] N. Kazantseva, U. Nowak, R. W. Chantrell, J. Hohlfeld, and A. Rebei, Slow recovery of the magnetisation after a subpicosecond heat pulse, Europhys. Lett. **81**, 27004 (2008).

[14] J. Mendil, Masters thesis, Georg-August-Universität, Göttingen, 2012.

[15] J. Mendil, P. Nieves, O. Chubykalo-Fesenko, J. Walowski, T. Santos, S. Pisana, and M. Münzenberg, Resolving the role of femtosecond heated electrons in ultrafast spin dynamics, Sci. Rep. **4**, 3980 (2014).

[16] A. V. Kimel, A. Kirilyuk, P. A. Usachev, R. V. Pisarev, A. M. Balbashov, and Th. Rasing, Ultrafast non-thermal control of magnetization by instantaneous photomagnetic pulses, Nature (London) **435**, 655 (2005).

[17] K. Vahaplar, A. M. Kalashnikova, A. V. Kimel, D. Hinzke, U. Nowak, R. Chantrell, A. Tsukamoto, A. Itoh, A. Kirilyuk, and Th. Rasing, Ultrafast Path for Optical Magnetization Reversal via a Strongly Nonequilibrium State, Phys. Rev. Lett. **103**, 117201 (2009).

[18] K. Vahaplar, A. M. Kalashnikova, A. V. Kimel, S. Gerlach, D. Hinzke, U. Nowak, R. Chantrell, A. Tsukamoto, A. Itoh, A. Kirilyuk, and Th. Rasing, All-optical magnetization reversal by circularly polarized laser pulses: Experiment and multiscale modeling, Phys. Rev. B **85**, 104402 (2012).

[19] D. A. Garanin, Generalized equation of motion for a ferromagnet, Physica (Amsterdam) **172A**, 470 (1991).

[20] R. F. L. Evans, D. Hinzke, U. Atxitia, U. Nowak, R. W. Chantrell, and O. Chubykalo-Fesenko, Stochastic form of the Landau-Lifshitz-Bloch equation, Phys. Rev. B **85**, 014433 (2012).

[21] M. I. Kaganov, I. M. Lifshitz, and L. V. Tanatarov, Relaxation between electrons and the crystalline lattice, Sov. Phys. JETP **4**, 173 (1957).

[22] P. Nieves Cordones, Ph.D. thesis, Instituto de Ciencia de Materiales de Madrid (ICMM)—Universidad Autónoma de Madrid, 2015.

[23] N. Kazantseva, D. Hinzke, U. Nowak, R. W. Chantrell, U. Atxitia, and O. Chubykalo-Fesenko, Towards multiscale modeling of magnetic materials: Simulations of FePt, Phys. Rev. B **77**, 184428 (2008).

[24] U. Atxitia, D. Hinzke, O. Chubykalo-Fesenko, U. Nowak, H. Kachkachi, O. N. Mryasov, R. F. Evans, and R. W. Chantrell, Multiscale modeling of magnetic materials: Temperature dependence of the exchange stiffness, Phys. Rev. B **82**, 134440 (2010).

[25] L. P. Pitaevskii, Electric forces in a transparent dispersive medium, Sov. Phys. JETP **12**, 1008 (1961).

[26] P. Oppeneer (to be published).

[27] P. Nieves, D. Serantes, U. Atxitia, and O. Chubykalo-Fesenko, Quantum Landau-Lifshitz-Bloch equation and its comparison with the classical case, Phys. Rev. B **90**, 104428 (2014).